Published in final edited form as:
*Mol Pharm*. 2008 ; 5(5): 891–897. doi:10.1021/mp800054w.

# Characterization and real-time imaging of gene expression of adenovirus embedded silk-elastinlike protein polymer hydrogels

**Arthur von Wald Cresce**[1,2,±], **Ramesh Dandu**[1,2,±], **Angelika Burger**[1,3,4], **Joseph Cappello**[5], and **Hamidreza Ghandehari**[1,2,4,6,*]

1*Department of Pharmaceutical Sciences, University of Maryland, Baltimore, Baltimore, MD, USA*

2*Center for Nanomedicine & Cellular Delivery, University of Maryland, Baltimore, Baltimore, MD, USA*

3*Department of Pharmacology and Experimental Therapeutics, University of Maryland, Baltimore, Baltimore, MD, USA*

4*Greenebaum Cancer Center, University of Maryland, Baltimore, Baltimore, MD, USA*

5*Protein Polymer Technologies, Inc., San Diego, CA, USA*

6*Departments of Pharmaceutics & Pharmaceutical Chemistry and Bioengineering, University of Utah, Salt Lake City, UT, USA.*

## Abstract

Transient expression levels, vector dissemination and toxicities associated with adenoviral vectors have prompted the usage of matrices for localized and controlled gene delivery. Two recombinant silk-elastinlike protein polymer analogs, SELP-47K and SELP-415K, consisting of different lengths and ratios of silk and elastin units, were previously shown to be injectable hydrogels capable of matrix-mediated controlled adenoviral gene delivery. Reported here is a study of spatio-temporal control over adenoviral gene expression with these SELP analogs in a human tumor xenograft model of head and neck cancer using whole animal imaging. Real-time images of viral expression levels indicate that polymer concentration and polymer structure are predominant factors that affect viral release and, thus viral transfection. Decrease in polymer concentration and increase in polymer elastin content results in greater release, probably due to changes in the network structure of the hydrogel. To better understand this relationship, macro and microstructural properties of the hydrogels were analyzed using dynamic mechanical analysis (DMA) and transmission electron microscopy (TEM). The results confirm that the concentration and the elastin content of the protein polymer affect the pore size of the hydrogel by changing the physical constraints of the SELP fibril network and the degree of hydration of the SELP fibrils. The potential to modulate viral release using SELP hydrogel delivery vehicles that can be injected intratumorally by minimally invasive techniques holds significant promise for the delivery of therapeutic viruses.

### Keywords

gene delivery; protein polymers; hydrogels; in vivo imaging; head and neck cancer

*To whom correspondence should be addressed: Hamidreza Ghandehari, PhD Departments of Pharmaceutics & Pharmaceutical Chemistry and Bioengineering University of Utah 383 Colorow Road, Room 343 Salt Lake City, Utah, 84108 Ph: 801 587−1566 Fax: 801−585−0575 Email: hamid.ghandehari@pharm.utah.edu.
±These authors contributed equally to this work

## 1. INTRODUCTION

Vector dissemination, transient gene expression and clearance from the site of action have been the Achilles' heel for the successful application of adenoviral vectors in preclinical cancer gene therapy (1,2). Intratumoral infusion of viral vectors has been applied with certain degree of success for tumor management (3). However, much needs to be done to prolong gene expression and enhance tumor localization to achieve desirable therapeutic outcomes. Matrix-mediated controlled delivery of viral vectors can address these issues and enhance the safety and efficacy of adenoviruses while minimizing their toxicities. Several particulate and depot based matrices have been utilized with varying degrees of success (4-7). Migration of the particulate systems and the limited availability of customizable biocompatible depot based systems severely undermine progress in this field (3,8,9).

Polymeric biomaterials used for localized controlled delivery are either derived from natural sources (e.g, collagen) or are chemically synthesized (e.g., poly(D,L-lactide-co-glycolide) (PLGA) and poly(vinyl alcohol) (PVA)). Recombinant DNA technology has made possible the exploitation of the cellular machinery (e.g, *E.coli*) for the synthesis of protein based polymers that may be inspired by nature but are not available naturally (10). Genetically engineered protein polymers combine the advantages of the biocompatibility and biodegradability of natural proteins on one hand with the control of polymer structure and function provided by chemically synthesized polymers on the other hand (11-14). DNA directed synthesis of these protein-based polymers allows unprecedented control over their sequence, structure and molecular weight, and thereby their physico-chemical properties that suit specific delivery needs (10,13). Of specific interest are silk-elastinlike protein polymers (SELPs), a class of genetically engineered polymers consisting of peptide repeats of silk-like (GAGAS) and elastin-like (GVGVP) units (10). The silk units provide physical cross linking capability whereas the elastin units confer aqueous solubility. By carefully controlling the ratio (s) and length(s) of silk and elastin units, SELPs of diverse functionalities (stimuli-sensitive, biocompatible and biodegradable) can be produced (15-18).

Solutions of two SELP analogs, 47K and 415K (Figure 1), with four silk units each and consisting of seven and fifteen elastin units, respectively and one elastin unit with a lysine (K) in the monomer repeat, are liquid at room temperature and undergo irreversible sol-to-gel transition at 37°C. Despite the differences in the length of the monomer repeats the molecular weight (length) of these analogs were kept fairly constant by precisely controlling the degree of multimerization using recombinant DNA methods (18). These protein polymers allow intratumoral injection of aqueous polymer-virus mixtures that transform into solid hydrogel matrices within minutes in the body, allowing localized matrix-mediated delivery of adenoviruses in the tumor mass. SELP-47K has been shown to localize and prolong transgene expression of plasmid DNA (19) or viruses (20) in murine xenograft models. We have further demonstrated that the structural analog of SELP-47K with longer elastin units but similar molecular weight, SELP-415K, has a lower shear modulus (18) and higher rate of viral release in vitro (21). However, the spatial and temporal control over SELP-mediated adenoviral gene expression *in vivo* is unknown. Further, limited information is available about the microstructure, the pore size of these networks and their mechanical properties. This is the first report of SELP-mediated spatial and temporal control over adenoviral gene expression, *in vivo*, as a function of polymer structure and composition. Also briefly reported are the influences of polymer composition on the mechanical properties of the hydrogel using dynamic mechanical analysis (DMA) and on the nano-fibrillar structures using transmission electron microscopy (TEM).

## 2. EXPERIMENTAL SECTION

### Materials

SELP-47K and SELP-415K solutions at 12wt% were obtained from Protein Polymer Technologies, Inc. (San Diego, CA). SELP-415K was biosynthesized and characterized by procedures described previously (18). SELP-47K is a protein block co-polymer composed of silk and elastin-like amino acid peptide motifs, with 12 repeating units, and a MW of 69,814 Da (22). Each repeating unit consists of series of four silk-like amino acid sequence blocks (GAGAGS) and eight elastin-like blocks (VPGVG, including one lysine-substituted elastin-like block, VPGKG). SELP-415K is composed of the same amino acid sequence blocks as SELP-47K except with eight more elastin blocks in each repeating unit. SELP-415K has 8 repeating units and a MW of 71,500 Da (18). Ad-CMV-Luc, a replication-defective human adenovirus Type 5 (dE1/E3) containing a firefly luciferase reporter gene under the control of the CMV promoter, was purchased from Vector Biolabs (Philadelphia, PA). 4−6 week old female athymic nu/nu mice purchased from Harlan (Indianapolis, IN) were used for the animal studies in accordance with the Institutional Animal Care and Use Committee (IACUC) at the University of Maryland, Baltimore. HN12 cells (Human squamous cell carcinoma cells of head and neck) were sub-cultured in Dulbecco's Modified Eagles Medium (DMEM) with 10% bovine serum albumin and 1% pencillin/streptomycin and used for establishing xenografts.

### In vivo Imaging Studies

HN-12 xenografts were established by subcutaneously injecting $1 \times 10^6$ cells suspended in 300ul of PBS on the left flank of 45 athymic nude mice. Tumors were allowed to grow for two weeks to reach an average diameter of 0.5 cm and were then randomized into 5 treatment groups (n=9 animals/group). A dose of $5 \times 10^8$ PFU of Ad-CMV-Luc was administered to the mice either alone or along with one of the three polymer compositions (4wt% SELP-47K, 10.9wt% SELP-47K, and 10.9wt% SELP-415K). PBS was administered to negative control animals. Virus-polymer solutions were prepared by thawing 12 wt% SELP and virus stocks and mixing them gently with PBS resulting in the dilution of the solutions to 10.9 wt% or 4 wt% protein polymer. Mice were anesthetized using isoflurane/$O_2$ (inhalation) and were injected intratumorally with a 50 μL dose of PBS, virus alone or along with one of the three different SELP compositions. Prior to collecting the imaging data, firefly luciferin (150 mg/kg) in PBS was administered by the intraperitonial route to each mouse. Luciferin acts as a substrate for the enzymatic oxidation, in the presence of the transgene (luciferase), to produce oxyluciferin and light which is captured by the whole-body imaging system (Xenogen IVIS 200). Spatio-temporal intensity of luminescence marked the location of transfection events within the mouse and in the tumor xenograft. Real-time imaging was carried out on mice anesthetized by isofluorane every 5 minutes over a 30 minute period to obtain the images and the data was analyzed using IVIS imaging software.

### Dynamic Mechanical Analysis (DMA)

DMA was carried out using TA Instruments DMA Q800. SELP hydrogels cylindrical in shape with a thickness of 4.2 mm and diameter of 19.2 mm were prepared by incubating at 37°C for 4 hours using methods described previously (19). Frequency ramp tests were performed by increasing the strain oscillation rate from 1 Hz to 100 Hz. Tests were performed isothermally at room temperature with a preload force of 0.01 N, on the sample in PBS, using a submersion clamp. 8 wt% and 12 wt% SELP-47K, as well as 12 wt% SELP-415K, were subjected to a constant 1% strain during the test. 4 wt% SELP-47K, was tested at 0.5% strain due to its lower mechanical strength.

### Transmission Electron Microscopy (TEM)

Hydrogels of four different compositions 4 wt%, 8 wt%, and 12 wt% of SELP-47K and 12 wt % of SELP-415K were made by curing the polymer at 37°C for 4 hours as described previously (19). Samples for electron microscopy were stained with osmium tetroxide ($OsO_4$), embedded in epoxy and ultramicrotomed to 100 nm thickness. Ad-CMV-Luc samples were prepared by placing a 10 μL drop of Ad-CMV-Luc solution onto a copper grid with a 50 nm carbon support film and negatively stained for 30 seconds with a 10 μL drop of 1% aqueous uranyl acetate ($C_4H_6O_6U \cdot 2H_2O$). Electron microscopy was performed on a JEOL JEM 2100 LaB6 transmission electron microscope operating at 200 kV. Images were captured using an integrated CCD camera.

## 3. RESULTS AND DISCUSSION

### Spatio-Temporal Localization of Transfection

4wt% SELP-47K was previously shown to be capable of prolonging the duration of adenoviral transgene expression up to 15 days in a xenograft model (20). Florescence microscopy of tumor sections revealed higher levels of transfection and localization within the tumor when delivered with SELP-47K. While it provided a proof of concept of SELP-mediated controlled gene delivery within the tumor, little is known about the transfection events surrounding the tumors and adjacent organs. The current study aims at tracking the transfection events in real time by using minimally invasive live animal imaging in place of the more traditional protein bioassays and tissue sectioning. This allowed repeated measurements of transfection events in the same animals. Intraperitonial injection of luciferin minutes prior to the test results in its distribution throughout the body allowing real-time imaging for transfection using the Xenogen IVIS 200. Whole animal imaging provided insight on the spatio-temporal localization of expression within and outside the tumor as well as adjacent organs.

Luminescence intensity images on day 1 (Figure 2; **Day 1**) indicate that 4wt% SELP-47K (Figure 2; **Day 1C**) has higher levels of transfection compared to the virus control (Figure 2; **Day 1B**) and all the other SELP compositions. Tumors of PBS control treated animals exhibited no luminescence indicating a lack of background signal. Within the SELP-virus compositions luminescence intensities were in the order of 4wt% SELP-47K > 10.9wt% SELP-415K > 10.9wt% SELP-47K. These results corroborate the viral release profiles of SELP analogs observed previously, with higher release observed at lower SELP-47K polymer compositions presumably resulting from a more loosely crosslinked hydrogel network allowing a greater initial release of the virus (21). The higher release observed in SELP-415K correlates with the presence of longer elastin units in the polymer structure allowing formation of a matrix with larger pore size (18,21).

Luminescence intensity in the 4 wt% SELP-47K group peaked by day 2 and then dropped sharply for the remainder of the study, as the initial release tapered off. Whereas in case of the 10.9wt% compositions of SELP-47K and to a greater extent SELP-415K, expression levels gradually rose throughout the study. This indicates SELP hydrogel compositions exert control over both the duration and the amount of viral release over time. Both these compositions produced expression within the tumor for the entire test. Expression levels peaked at day 9 and day 15 respectively for the 10.9 wt% composition of SELP-47K and -415K, but at different intensity levels. The higher level of expression with SELP-415K at the same polymer concentration indicates that the matrix is more permissive of viral release than SELP-47K. While localization of expression was observed in the case of the virus alone as well as the 4wt % SELP-47K group, initially, by day 9 expression began to be detected outside the boundaries of the tumor and in the trunk of the mouse (Figure 2; **Day 9B and 9C, Day 15B and 15C**).

These observations made *in vivo* along with previous observations examining *in vitro* release as a function of polymer structure (21), provide insight on the controlled release of adenoviruses from SELP matrices. However, little is known about how SELP microstructure and the mechanical properties of the hydrogel impact viral release and subsequent transfection *in vivo*. A brief investigation of pore structure and mechanical properties of SELP hydrogels by dynamic mechanical analysis (DMA) and transmission electron microscopy (TEM) was carried out to correlate these parameters with viral release and transfection.

## Dynamic Mechanical Analysis (DMA)

Previous studies with SELPs suggest that the cross linking density is a function of polymer concentration, structure and cure time (18,22). Since mechanical properties of hydrogels are largely governed by cross linking density, DMA of SELPs was carried out at different polymer compositions (structure and concentration) at constant cure time. While aware of the probable changes in mechanical properties with cure time and cure temperature we restricted our analysis to samples cured for 4 hours at 37° C to allow comparison with previous swelling and release data (18,21,22). The storage modulus (stiffness) and loss modulus (dampening and energy dissipation) of SELP hydrogels was analyzed in compression using DMA to delineate the viscoelastic behavior. As expected for the SELP-47K compositions, storage modulus was directly related to concentration, 4 wt% (◆) < 8 wt% (■) < 12 wt% (▲) (Figure 3). These observations are consistent with previous observations indicating that the distance between the physical crosslinks of the SELP hydrogel network decrease with increase in concentration from 4 wt% to 12 wt% cured for 4 hours. The storage modulus of 4 wt% SELP-47K was 75.4 kPa while that of 12 wt% SELP-47K was 1600 kPa. At 4 wt%, SELP-47K hydrogels were translucent, soft and easily deformed, whereas at 12 wt%, they were opaque and firm during handling. Interestingly, 12 wt% SELP-415K hydrogels gave storage modulus values similar to those of 4 wt% SELP-47K, about 70 kPa. SELP-415K 12 wt% hydrogel was opaque, white, and more flexible than 12 wt% SELP-47K hydrogel.

The *in vivo* viral release results should correlate with the physical structure of the SELP hydrogels. However, it is important to note that *in vivo* these hydrogels cure progressively at 37°C, and ultimately for longer periods than the samples tested *in vitro* (4 hour cure time). 4wt % SELP-47K hydrogel produces a soft network with a low density of crosslinks, as indicated by its relatively low storage modulus (stiffness). This hydrogel allows an initial burst release of the virus early on (Figure 2, **Day 1C and Day 2C**). At higher concentrations SELP-47K hydrogel produces a stiffer network with a greater crosslinking density (greater storage modulus), and initial virus release is significantly reduced (Figure 2, **Days 1D-5D**).

Despite similar storage moduli for 12 wt% SELP-415K and 4 wt% SELP-47K hydrogels, SELP-415K results in more consistent viral release and localization of transfection. This may be due to the difference in polymer structure. SELP-415K contains sixteen elastin-like sequence blocks in its repeat unit (the K unit is a lysine-substituted elastin block). SELP-47K has eight. Hydrogen bonding of the silk-like blocks is assumed to be responsible for physical crosslinking of SELPs (13). Both polymers have the same number of beta-sheet forming silk-like blocks per repeat (four). SELP-415K and SELP-47K have silk-like block contents of 0.25 and 0.33, respectively. Therefore based simply on composition, a solution of SELP-415K would need to be approximately 1.3 times the concentration of a solution of SELP-47K to yield the equivalent concentration of silk-blocks. Yet, comparable storage moduli are obtained with an SELP-415K concentration of approximately 3 times that of SELP-47K (12 wt% vs 4 wt%).

Apparently, a combination of factors in addition to the effective concentration of silk-like blocks must influence the mechanical properties of the hydrogel network. The separation of the silk units by longer elastin repeats in SELP-415K could increase the distance between physical crosslinks by a factor of 8 in a three-dimensional network as compared to SELP-47K.

Additionally, the extended elastin repeats could decrease the rate and extent of formation of the necessary beta-sheets that stabilize the 3-dimensional network.

### Transmission Electron Microscopy (TEM)

Transmission electron microscopy (TEM) was employed to examine the microstructure of SELP hydrogels of different composition. It is known that silk-like blocks will form hydrogen-bonded antiparallel β-sheets under certain aqueous conditions (23-25). The association of adjacent SELP chains in these beta-sheets is the presumed basis for the physical crosslinking that binds together the hydrogel structure.

TEM images (Figure 4) show that there is a clear decrease in network spacing as the concentration of SELP-47K increases. For comparison, an image of the Ad-CMV-Luc virion is included in Figure 4A-inset, showing the virus particle to be approximately icosahedral (hexagonal when viewed in 2-D) with a diameter of 22 nm. 4 wt% SELP-47K hydrogels displayed a relatively open microstructure, with well-defined fibrils spaced about 93 nm apart on average, although there was a great degree of variation in fibril spacing that made the description of the average fibril spacing difficult. This distance between adjacent fibrils is consistent with the low storage modulus of 4 wt % SELP-47K hydrogel observed in DMA and may explain the burst release of viruses observed in vivo (Figure 2; **Day 1C**) .

12 wt% SELP-47K (Figure 4B) had significantly shorter distances between fibrils, a result consistent with its storage modulus nearly 2 orders of magnitude greater than 4 wt% SELP-47K. The smaller average fibril spacing at 31 nm would predict lesser virus release due to the physical barrier of a tighter network in comparison to 4 wt% SELP-47K.

In comparison to the well-defined fibrils observed in SELP-47K hydrogels, SELP-415K fibrils were difficult to image by TEM, and appeared poorly defined, thicker and less regular (Figure 4C). Therefore, it was not possible to determine an accurate interfibril distance by TEM. However, based on the in vivo viral expression images which indicated that SELP-415K confined viral transfection to within the tumor while promoted a longer and more consistent release of virus, it is expected that the SELP-415K hydrogel network would have a relatively tight interfibril spacing yet accommodate substantial viral movement.

## 5. CONCLUSION

Results from *in vivo* studies as well as *in vitro* characterizations indicate that polymer concentration and structure are two predominant factors governing adenoviral release from SELP protein polymer hydrogels. Increasing the hydrogel polymer concentration caused an increase in the storage modulus (stiffness), a decrease in interfibril distance, and a corresponding decrease in viral release. Changing the structure of the polymer by increasing the length of the elastin-like repeating units caused a decrease in the storage modulus and an increase in viral release over a greater duration.

These studies taken along with previous work (19-21) highlight the capability of SELPs as matrices for localized controlled delivery of adenoviruses. The spatio-temporal control over transfection qualitatively shown here holds promise for the evaluation of the efficacy of SELP-mediated delivery of therapeutic viruses to accessible, localized tumors such as head and neck cancers. Additionally, results presented here provide preliminary visual evidence of the nanostructure of self-assembled SELP polymers and their influence on physico-mechanical behavior (stiffness and porosity) that govern release from these polymeric matrices. The minimally invasive technique of intratumoral injection of polymer-virus solutions to form hydrogel matrices, *in situ*, obviates the need for physical implantation that is required for a number of other depot-based delivery systems. The next logical steps in these studies are the

quantitative evaluation of viral biodistribution and transfection using quantitative/real-time PCR (qPCR/RT-PCR) and evaluating these systems in tumor treatment.

## 5. ACKNOWLEDGEMENT

We are very grateful to Dr. Stuart Martin of the Department of Physiology at the University of Maryland, Baltimore, for training and advice in the use of the Xenogen IVIS 200 imaging machine. Use of the DMA was graciously provided by Dr. Peter Kofinas of the Bioengineering Department of the University of Maryland, College Park. Dr. Wen-An Chiou provided access to the electron microscope facility at the NISPLab of the University of Maryland, College Park, and provided help in capturing and interpreting images. Funding for this study was provided under NIH R01 CA107621.

## 6. Abbreviations

Ad-CMV-Luc, Human adenovirus with a firefly luciferase gene and CMV promoter; DMA, Dynamic Mechanical Analysis; DMEM, Dulbecco's Modified Eagles Medium; GAGAS, Glycine-Alanine-Glycine-Alanine-Serine (silk motifs); GVGVP, Glycine-Valine-Glycine-Valine-Proline (elastin motifs); PLGA, Poly(D,L-lactide-co-glycolide) (PLGA); PVA, Poly (vinyl alcohol); SELP, Silk-elastinlike protein polymer; TEM, Transmission Electron Microscopy; qPCR/RT-PCR, Quantitative/real-time polymerase chain reaction.

## References

1. Verma IM, Somia N. Gene therapy -- promises, problems and prospects. Nature 1997;389(6648):239–242. [PubMed: 9305836]
2. Everts M, Curiel DT. Transductional targeting of adenoviral cancer gene therapy. Curr.Gene Ther 2004;4(3):337–346. [PubMed: 15384947]
3. Wang Y, Hu JK, Krol A, Li YP, Li CY, Yuan F. Systemic dissemination of viral vectors during intratumoral injection. Mol.Cancer.Ther 2003;2(11):1233–1242. [PubMed: 14617797]
4. Beer SJ, Matthews CB, Stein CS, Ross BD, Hilfinger JM, Davidson BL. Poly (lactic-glycolic) acid copolymer encapsulation of recombinant adenovirus reduces immunogenicity in vivo. Gene Ther 1998;5(6):740–746. [PubMed: 9747453]
5. Doukas J, Chandler LA, Gonzalez AM, Gu D, Hoganson DK, Ma C, et al. Matrix immobilization enhances the tissue repair activity of growth factor gene therapy vectors. Hum.Gene Ther 2001;12(7): 783–798. [PubMed: 11339895]
6. Gersbach CA, Coyer SR, Le Doux JM, Garcia AJ. Biomaterial-mediated retroviral gene transfer using self-assembled monolayers. Biomaterials 2007;28(34):5121–5127. [PubMed: 17698189]
7. Levy RJ, Song C, Tallapragada S, DeFelice S, Hinson JT, Vyavahare N, et al. Localized adenovirus gene delivery using antiviral IgG complexation. Gene Ther 2001;8(9):659–667. [PubMed: 11406760]
8. Wang Y, Li CY, Yuan F. Systemic virus dissemination during local gene delivery in solid tumors and its control with an alginate solution. Conf.Proc.IEEE Eng.Med.Biol.Soc 2004;5:3524–3526. [PubMed: 17271050]
9. Paielli DL, Wing MS, Rogulski KR, Gilbert JD, Kolozsvary A, Kim JH, et al. Evaluation of the biodistribution, persistence, toxicity, and potential of germ-line transmission of a replication-competent human adenovirus following intraprostatic administration in the mouse. Mol.Ther 2000;1 (3):263–274. [PubMed: 10933942]
10. Cappello J, Crissman J, Dorman M, Mikolajczak M, Textor G, Marquet M, et al. Genetic engineering of structural protein polymers. Biotechnol.Prog 1990;6(3):198–202. [PubMed: 1366613]
11. Haider M, Megeed Z, Ghandehari H. Genetically engineered polymers: status and prospects for controlled release. J.Control.Release 2004;95(1):1–26. [PubMed: 15013229]
12. Dandu R, Ghandehari H. Delivery of bioactive agents from recombinant polymers. Progress in Polymer Science 2007;32(8−9):1008–1030.
13. Ghandehari H. Recombinant biomaterials for pharmaceutical and biomedical applications. Pharm Res 2008;25(3):672–673. [PubMed: 17710512]

14. McGrath K, Tirrell DA, Kawai M, Mason TL, Fournier MJ. Chemical and biosynthetic approaches to the production of novel polypeptide materials. Biotechnol.Prog 1990;6(3):188–192. [PubMed: 1366612]
15. Dinerman AA, Cappello J, Ghandehari H, Hoag SW. Solute diffusion in genetically engineered silk-elastinlike protein polymer hydrogels. J.Control.Release 2002;82(2−3):277–287. [PubMed: 12175743]
16. Megeed Z, Cappello J, Ghandehari H. Controlled release of plasmid DNA from a genetically engineered silk-elastinlike hydrogel. Pharm.Res 2002;19(7):954–959. [PubMed: 12180547]
17. Nagarsekar A, Crissman J, Crissman M, Ferrari F, Cappello J, Ghandehari H. Genetic engineering of stimuli-sensitive silk-elastinlike protein block copolymers. Biomacromolecules 2003;4(3):602–607. [PubMed: 12741775]
18. Haider M, Leung V, Ferrari F, Crissman J, Powell J, Cappello J, et al. Molecular engineering of silk-elastinlike polymers for matrix-mediated gene delivery: biosynthesis and characterization. Mol.Pharm 2005;2(2):139–150. [PubMed: 15804188]
19. Megeed Z, Haider M, Li D, O'Malley BW Jr. Cappello J, Ghandehari H. In vitro and in vivo evaluation of recombinant silk-elastinlike hydrogels for cancer gene therapy. J.Control.Release 2004;94(2−3):433–445. [PubMed: 14744493]
20. Hatefi A, Cappello J, Ghandehari H. Adenoviral gene delivery to solid tumors by recombinant silk-elastinlike protein polymers. Pharm.Res 2007;24(4):773–779. [PubMed: 17308969]
21. Dandu R, Cappello J, Ghandehari H. Characterization of structurally related adenovirus-laden silk-elastinlike hydrogels. J. Bioact. Compt. Pol 2008;23:5–19.
22. Dinerman AA, Cappello J, Ghandehari H, Hoag SW. Swelling behavior of a genetically engineered silk-elastinlike protein polymer hydrogel. Biomaterials 2002;23(21):4203–4210. [PubMed: 12194523]
23. Rauscher S, Baud S, Miao M, Keeley FW, Pomes R. Proline and glycine control protein self-organization into elastomeric or amyloid fibrils. Structure 2006;14(11):1667–1676. [PubMed: 17098192]
24. Xu M, Lewis RV. Structure of a protein superfiber: spider dragline silk. Proc.Natl.Acad.Sci.U.S.A 1990;87(18):7120–7124. [PubMed: 2402494]
25. Anderson JP, Cappello J, Martin DC. Morphology and primary crystal structure of a silk-like protein polymer synthesized by genetically engineered Escherichia coli bacteria. Biopolymers 1994;34(8):1049–1058. [PubMed: 8075387]

**A.**

MDPVVLQRRDWENPGVTQLNRLAAHPPFASDPMG**AGSGAGAGS**
**{(GVGVP)$_4$ GKGVP (GVGVP)$_3$ (GAGAGS)$_4$}$_{12}$ (GVGVP)$_4$ GKGVP**
**(GVGVP)$_3$ (GAGAGS)$_2$ GAG**AMDPGRYQDLRSHHHHHH

**B.**

MDPVVLQRRDWENPGVTQLNRLAAHPPFASDPMG**AGSGAGAGS**
**{(GVGVP)$_4$ GKGVP (GVGVP)$_{11}$ (GAGAGS)$_4$}$_7$ (GVGVP)$_4$ GKGVP**
**(GVGVP)$_{11}$ (GAGAGS)$_2$ GAG**AMDPGRYQDLRSHHHHHH

**Figure 1.**
The amino acid sequence of SELP analogues: (A) SELP-47K (molecular weight: 69,814 Da) and (B) SELP-415K (molecular weight: 71,500 Da). Polymer analogs were composed of head and tail portions and a series of silk (GAGAGS) and elastin-like (GVGVP) repeats with the primary repetitive sequences in bold, and positively charged amino acids (at pH 7.4) highlighted in gray.

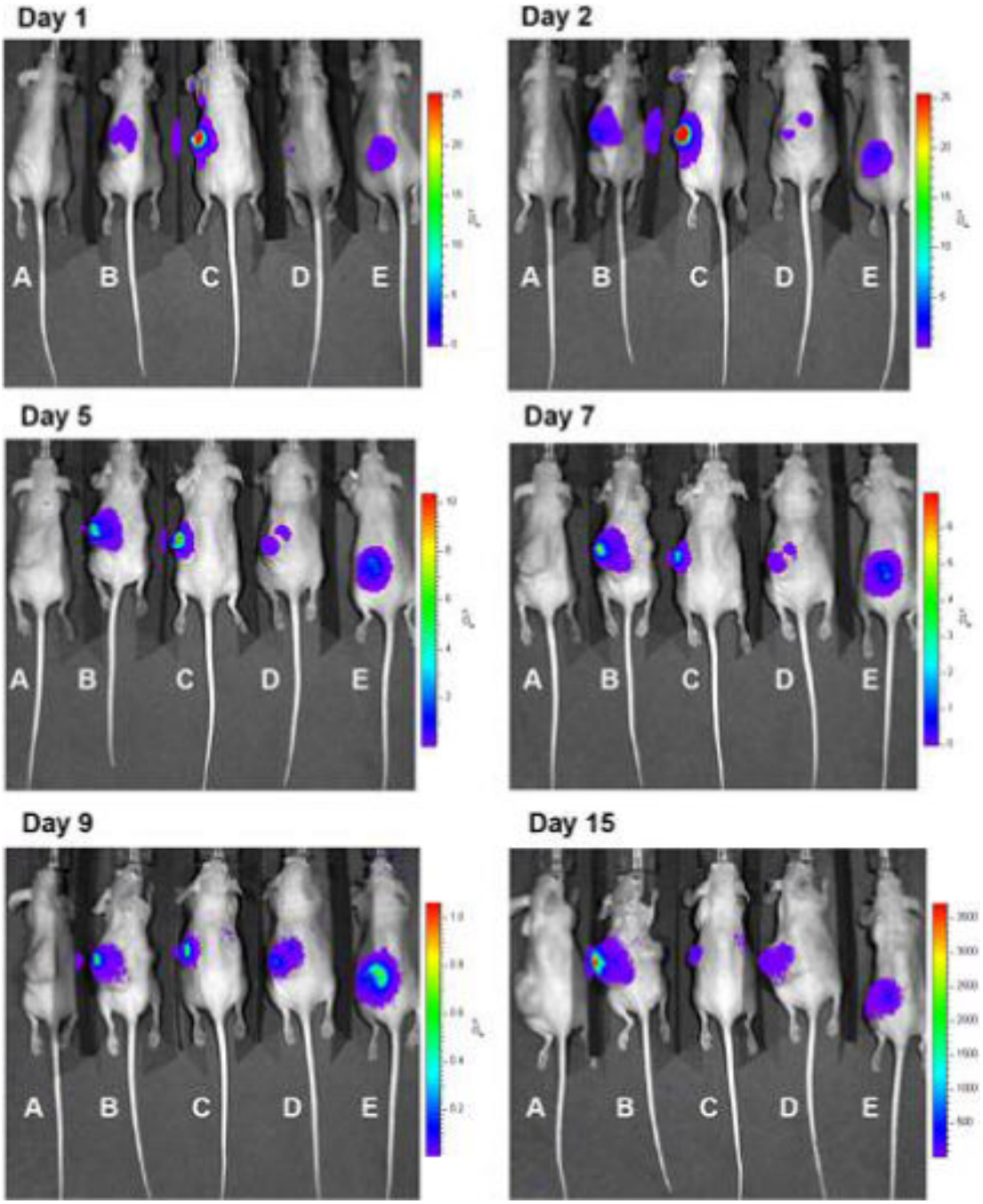


**Figure 2.**
Typical time course of luciferase expression in HN12 tumor xenografts in athymic nude mice. Mouse A: PBS control. Mouse B: Ad-CMV-Luc control. Mouse C: 4 wt% SELP-47K + Ad-CMV-Luc. Mouse D: 10.9 wt% SELP-47K + Ad-CMV-Luc. Mouse E: 10.9 wt% SELP-415K + Ad-CMV-Luc.

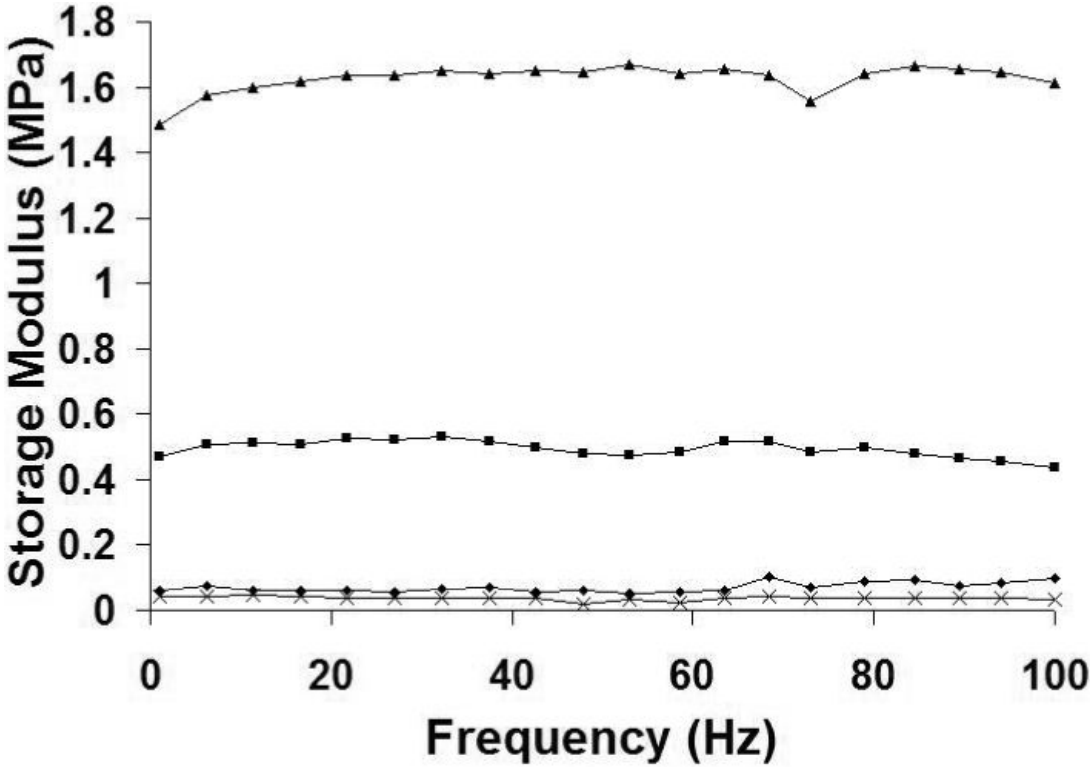


**Figure 3.**

Dynamic mechanical analysis of SELPs 47K 4 wt% (◆), 8 wt% (■), and 12 wt% (▲) as well as SELP-415K 12 wt% (×) cured for 4 hours. SELP-47K 12 wt% formed stiff gels that had significantly higher modulus than all other tested gels. SELP-415K 12 wt%, despite forming hydrogels that held their shape unaided, gave results similar to that of the weakest SELP-47K 4 wt% hydrogels.

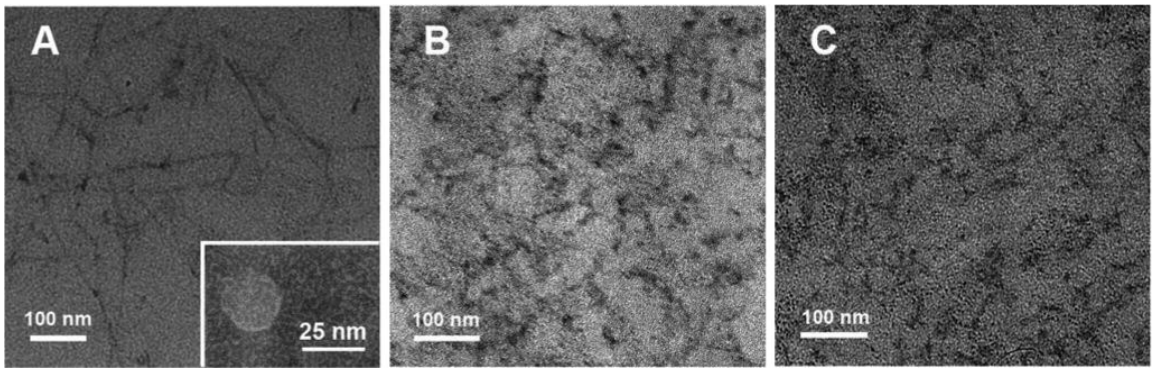


**Figure 4.**
Transmission electron microscope image of (A) 4 wt% SELP-47K, (inset) icosahedral Ad-CMV-Luc virion, (B) 12 wt% SELP-47K and (C) 12 wt% SELP-415K.